Film growth and wetting of curved surfaces

L. Wilen and E. Polturak
Department of Physics, The Technion-Israel Institute of Technology, Haifa 32000, Israel
(Received 30 January 1990)

We report experiments on the low-temperature adsorption of ^{4}He films on the surface of graphite fibers. We contrast the adsorption on two kinds of fibers, one with a positive radius of curvature, and one for which part of the surface has a negative curvature. The curvature has a dramatic effect on the limiting thickness of the film. For the fiber with positive curvature, the limiting film thickness is less than 200 Å, while for the fiber with negative curvature it can reach over 10 000 Å. The data agree very well with the universal form of the Dzyaloshinskii, Lifshitz, and Pitaevskii [Adv. Phys. **10**, 165 (1961)] theory as worked out by Cheng and Cole [Phys. Rev. B. **38**, 987 (1988)]. This agreement, though, may perhaps be fortuitous as the convoluted surface of the fiber gives rise to an adsorption process that is more complex than what this theory describes.

INTRODUCTION

Considerable interest has arisen in past years in the nature of wetting of solid substrates by liquid and solid films.[1–4] The ability of a film to wet a surface is characterized by the strength of the substrate-adsorbate interaction. Wetting can be inhibited for interactions which are either too small or too large, and a rich variety of phase diagrams was predicted for various degrees of wetting of the substrate by the adsorbate.[2,4] The details of adsorption in systems which wet completely are thought to be well understood theoretically in the framework of the theory developed by Dzyaloshinskii, Lifshitz, and Pitaevskii (DLP).[5] This theory fully accounts for retardation effects in the van der Waals interaction which are important for thick films. The DLP theory was verified in a convincing fashion by Sabisky and Anderson[6] for helium adsorption on various atomically flat substrates over a wide range of film thicknesses. Very little work has been done is other helium-substrate systems to look at film growth in the retarded regime. One reason is that, for porous substrates, capillary condensation can preclude the observation of the continuous growth of thick films.[7] Even for nonporous materials, surface morphology can complicate the details of the adsorption process.[8]

In recent years, Bartosch and Gregory[9] introduced an elegant adsorption technique using a thin vibrating graphite fiber as a microbalance. The graphite fiber substrate has the advantages that it is nonporous, in the sense that there are no regions where irreversible capillary condensation occurs, and it can be cleaned *in situ*. Moreover, fibers of varying surface structure are available. Several experiments were performed with this technique using a variety of gases (O_2, Ar, ^{4}He).[9–11]

These experiments were all analyzed using the Frenkel-Halsey-Hill (FHH) theory,[12] which is essentially the limit of the DLP theory where retardation is neglected. For thick enough films, retardation and curvature become the dominant factors determining the film growth. Therefore a quantitative study of the effect of these two factors is of importance.

In the present experiment we carry out such a study. In order to access the thick-film region, one must work at pressures extremely close to the saturated vapor pressure. To realize this, we adopted a technique where the fiber is located near the top of a long (10-cm) cell. In this way, when liquid begins to form at the bottom of the cell, the fiber is at a pressure smaller than the saturated pressure by the amount ρgh. This very small distance from the phase boundary can be conveniently manipulated by changing the liquid level in the cell. For example, at 2K and with $h = 1$cm, the pressure difference from saturated conditions is less than 10^{-3} mm Hg. This amounts to $\sim 3\times 10^{-5}$ of the saturated vapor pressure.

Furthermore, we study two types of fiber, one with the usual round cross section, and a more exotic type, with a cross section having a region of negative curvature. By contrasting these two varieties, we can draw meaningful conclusions regarding the effect of surface morphology on the adsorption process.

In particular, we show that complete wetting takes place by demonstrating continuous film growth up to a thickness of 10 000 Å. On the other hand, we show that there is a contradiction involved in the straightforward application of the DLP theory to describe film growth on a highly convoluted surface. In fact, it is quite surprising that the theory can actually fit the data as well as it does.

CHARACTERIZATION OF FIBERS

We turn now to a brief discussion of the nature of the two fibers used in the experiment. Figure 1 shows electron micrographs of the two fibers. The P-100 fiber,[13] shown in Fig. 1(a), is a circular pitch-based graphite fiber whose basal planes run along the axis. The size of the crystal domains has been estimated to be about 200 Å, based on work on x-ray line broadening.[11] As discussed in previous work, one effect of the surface structure is to provide extra area for adsorption.[10]

The Fortafil 5 fiber,[14] shown in Fig. 1(b) is unique in its noncircular cross section, which resembles a figure 8. It is clearly seen that the fiber has regions of both positive

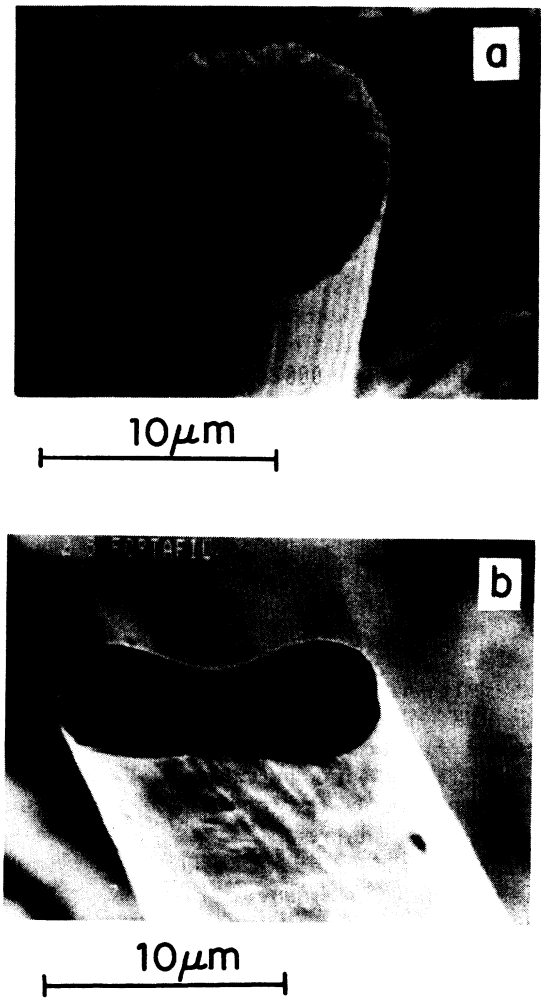

FIG. 1. Scanning electron microscope cross-sectional photographs of the two fibers used in the experiment. (a) P-100 fiber. (b) Fortafil fiber.

and negative curvature. On a smaller scale, some wavy ridgelike features are evident, although we do not believe that they reflect any underlying crystal structure. From resistivity and isothermal adsorption measurements we can conclude that this fiber is amorphous carbon with domain size probably at most 10 Å.

EXPERIMENTAL SETUP

The experimental arrangement is shown in Fig. 2. A capacitor is formed by two vertical parallel plates of printed circuit board. The electrode arrangement is such that fringing fields are eliminated. The capacitor serves to measure the gas density in the cell below saturation, and also to measure the level of bulk helium in the cell, as it is filled at the saturated vapor pressure. The capacitor is read using a standard three-terminal bridge. We can resolve about 10^{-5} pF which corresponds to a density resolution of 1.6×10^{-6} g/cm^3. At 2K, this is two parts in 10^3 of the total density of the saturated vapor. When

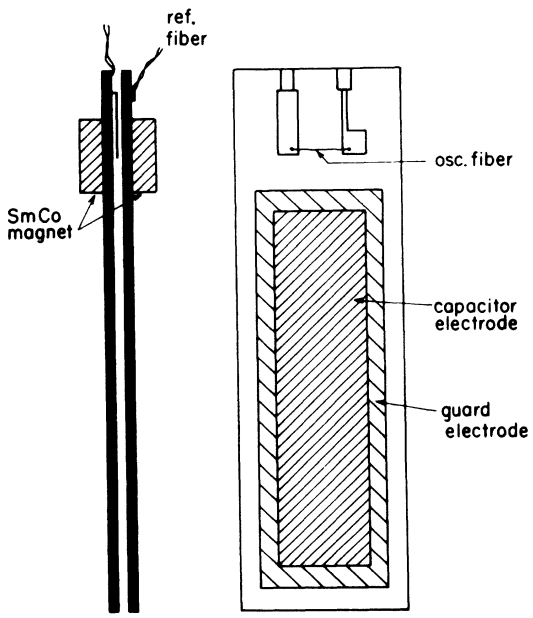

FIG. 2. Schematic representation of the experimental cell.

measuring the height of bulk liquid helium in the cell, the resolution in capacitance translates to a resolution of 0.001 mm in the level.

Above the capacitor, a graphite fiber of length approximately 1 cm is attached horizontally between two thin strips of phosphor bronze, one of which serves as a spring to hold the fiber under constant tension. This fiber is the oscillating microbalance. The fundamental resonant frequency is about 10 kHz. The Q of the fiber in vacuum was $\sim5\times10^4$ at a temperature of 2 K, and decreased to about 10^3 when the density of the gas surrounding the fiber reached saturation. Centered about the fiber on the outside of the plates are two permanent magnets whose field is perpendicular to the fiber. A reference graphite fiber, of the same resistance as the oscillator, is varnished to the outside of one of the capacitor plates. The oscillator and reference fibers constitute two arms of an ac Wheatstone bridge. Placing the reference fiber near the oscillator fiber has the advantage that the resistance of the fiber oscillator is almost perfectly balanced by the resistance of the reference fiber, independent of temperature. The inductive component of the voltage across the oscillating fiber, caused by its motion in the magnetic field, is used in a phase-locked loop arrangement to maintain the resonant condition. The power dissipation in the fiber was always kept <50 pW and the resonant frequency was experimentally independent of drive at these levels.

The copper sample cell, containing the capacitor, fibers, and magnets, was immersed in a pumped helium bath. The temperature of the bath was electronically controlled to within 1mK. The experiments reported here were carried out at $1.2\text{ K} < T < T_\lambda$.

Before a run, we heated the fiber *in situ* to a temperature of 1000°C (with the cell at <2K) to burn off any contaminants. The temperature was determined by

measuring the fiber resistance during heating. The dependence of the fiber's resistance on temperature had been measured previously.

Both the resonance frequency and capacitance signals were automatically monitored at intervals of 20 sec as helium gas was allowed to leak slowly into the cell. A typical run from $\rho=0$ to $\rho=\rho_{\text{sat}}$ took ~ 3 h. Once saturation was achieved, helium was added and a similar procedure was followed to obtain the resonant frequency as the bulk liquid level increased.

Periodic checks were made to ensure that the adsorption process was reversible. This is important to rule out the occurrence of catastrophic capillary condensation. For conditions below saturation, we could pump on the cell and lower ρ to check that the data reproduced. For conditions at saturated vapor pressure, this was not possible, since the pumping rate was too slow to appreciably lower the bulk helium level in the cell over a reasonable length of time.

For this region, we checked for reversibility in the following way: By letting in a small quantity of helium quickly, we could overpressure the cell to a pressure infinitesimally close to the saturation pressure. When this was done, we noted that the frequency dropped to the value that was later obtained, just before the bulk liquid covered the fiber. After a few seconds, the frequency would return to its value before the helium was introduced, as the excess gas condensed. (The quantity of gas let into the cell, in this case, was too small to produce a measurable frequency change, if introduced slowly.) This test was performed at various points along the curve, and no evidence for hysteresis was ever observed.

THEORY

Cheng and Cole[15] have worked out the DLP theory for film growth of various liquids on various substrates, and have cast the results in a universal form. They determine the van der Waals constant $\gamma(d)$ by the relation

$$\gamma(d)=\gamma(0)[1+1.64(d/d_{1/2})^{1.4}]^{-1/1.4} , \tag{1}$$

where d is the film thickness. $\gamma(0)$ and $d_{1/2}$ are functions of the adsorbate and substrate, and for helium on graphite are given to be

$$\gamma(0)=1890\ \text{K}\,\text{Å}^3 ,$$

$$d_{1/2}=180\ \text{Å} .$$

Retardation effects are contained in the dependence of $\gamma(d)$ on d. The film thickness is now determined by equating chemical potentials inside and outside of the film:

$$\frac{\gamma(d)}{d^3}=k_B T\left[\left(1+\frac{2B\rho_l}{m}\right)\ln\frac{\rho}{\rho_0}+\frac{mgh}{k_B T}+\frac{\sigma v}{rk_B T}\right] . \tag{2}$$

Here, σ is the surface tension of the liquid, m is the molecular mass, v is the molecular volume, and r is the radius of the fiber. In the first term on the right-hand side, we have included a correction to the chemical potential of the vapor due to the nonideality of the vapor. (B is the virial coefficient, and ρ_l is the liquid density.)

The last term on the right-hand side of Eq. (2) refers to the effect of surface tension due to the curved surface of the film. The surface tension serves to either enhance (negative curvature) or inhibit (positive curvature) film growth. For positive curvature, the film thickness is limited to a maximum value defined by $\gamma(d)/d^3=\sigma v/r$. A negative curvature leads to a divergence of the film thickness at saturation ($\rho=\rho_0$) when $h=h_c=\sigma v/mgr$. In the present experiment, h is varied between 1 and 10 cm. In general, the effects of curvature are most evident when $mgh\sim\sigma v/r$. This means that the experiment is best suited for the study of fibers with radii of curvature in the range 2–20 μm. For the fibers we used, the curvature is precisely in that range.

For the purposes of comparing results from the two types of fiber to the predictions of the theory, it is most illustrative to plot data in the form $\log_{10}\Delta f$ versus $\log_{10}\Delta\mu'/kT$ where

$$\Delta\mu'=kT\left[1+\frac{2B\rho_l}{m}\right]\ln\frac{\rho}{\rho_0}+mgh . \tag{3}$$

This is also the natural choice for the x coordinate since $\Delta\mu'$, the difference of the chemical potential from its value at the phase boundary, is the parameter experimentally varied. The effective curvature of the fiber then becomes a parameter of the theory to be determined by fitting the experimental results.

In comparing the theory with experiment, we must relate the film thickness d to the shift in the resonant frequency from its value as measured in vacuum. The shift Δf_{tot} is comprised of two terms: Δf_h, caused by the hydrodyamic drag on the fiber by the surrounding vapor, and Δf_a, caused by adsorption. The frequency shift due to a film of thickness d and density ρ_l adsorbed on a circular fiber of radius r is given by

$$\frac{\Delta f_a}{f_0}=-\frac{\rho_l}{\rho_f}\frac{d}{r} , \tag{4}$$

where ρ_f is the fiber density, f_0 is the frequency of the fiber as measured in vacuum.

For a fiber of arbitrary cross section we can write

$$\frac{\Delta f_a}{f_0}=-\frac{1}{2}\frac{\rho_l A d}{m_f} , \tag{5}$$

where A is the effective surface area of the fiber and m_f is the mass of the fiber. It has been noted in other work that the effective surface area, which must be assumed in this equation to fit adsorption data, is always larger than the calculated geometric area, presumably due to the convoluted surface structure. In our work, we determine the ratio of effective to geometric surface areas as a parameter in our fit to the data, and simply note that we get values of ~ 3.5 for this ratio, independent of film thickness. This number is also similar to that found by Zimmerli and Chan, by a direct adsorption measurement on a large quantity of fibers.[10]

We now discuss the hydrodynamic contribution to Δf. The hydrodynamic problem was originally solved in a pa-

per by Stokes,[16] and determines that the frequency shift of a fiber of density ρ_f moving in a gas of density ρ_v is

$$\frac{\Delta f_h}{f_0} = -\frac{\kappa \rho_v}{\rho_f} , \tag{6}$$

where κ is a function of the dimensionless parameter q given by

$$q = \frac{r}{2\delta} . \tag{7}$$

Here $\delta = (\eta/\omega\rho_v)^{1/2}$ is the viscous penetration depth, η is the viscosity of the vapor, and r is the radius of the fiber. For a circular fiber, κ is a known function as worked out by Stokes. For a noncircular fiber, such as the Fortafil, κ can only be solved for numerically. In the limit that $\delta \ll r$, κ is a constant, whose value depends only on the fiber geometry. In this case, the hydrodynamic frequency shift would be a linear function of the vapor density. For our system, $\delta \sim r$, and the dependence on the density is more complicated.

In order to correctly analyze the effects of adsorption, the background contribution to Δf due to hydrodynamics must be subtracted. This is especially critical at low coverages where the adsorption contribution is small. This contribution cannot be calculated exactly. However, we can obtain an experimental curve for the background by taking advantage of the fact that at saturation, the adsorbed film thickness is independent of temperature. By varying T (at saturation), we can sweep the saturated vapor pressure p_v (and hence ρ_v) over the same range for which the adsorption data were taken. Since no adsorption takes place during this process, recording Δf versus ρ_v then yields a background curve which is due to the hydrodynamics alone.[17] In Fig. 3, we show typical data of frequency versus density and the data used for background subtraction.

The background data can only be determined up to an overall additive constant. This constant is fixed by demanding that the difference between the two curves, which represents the frequency shift due to adsorption, will obey the FHH theory. We apply this condition to the data in the regime of low film coverage where retardation and curvature effects are negligible. A similar procedure was followed by others.[10] Henceforth in our discussion, we will refer to Δf as the part of the frequency shift due to adsorption alone.

RESULTS AND DISCUSSION

In Fig. 4, we plot data from both fibers in the form Δf versus $\Delta\mu'/kT$. As is seen, there are two regions in $\Delta\mu'$ where data were obtained. The points in the range $-0.5 > \log_{10}\Delta\mu' > -3.0$ correspond to the unsaturated vapor pressure regime, while those for which $-3.5 > \log_{10}\Delta\mu' > -5.0$ were obtained as the level of helium in the cell increased at saturated vapor pressure. The gap in the data is in the region $p_0 > p > 0.998p_0$ and is due to the finite resolution of our pressure measurement.

For the sake of comparison, the data in Fig. 4 span only four orders of magnitude in $\Delta\mu'/kT$. For the Fortafil fiber, we have obtained data spanning seven orders of magnitude.

It is clear from Fig. 4 that the data for both fibers look very similar in the unsaturated vapor pressure region. The effects of curvature become important only very near the saturation conditions which are realized in our experiment while the cell is gradually filled with liquid. The figure shows clearly that the adsorption characteristics in the saturated region are very different for the two fibers, in a way which is qualitatively what one would expect based on their different curvatures.

In Fig. 5 we plot data from the P-100 fiber, along with the fit that we obtained using the full theory with both retardation and curvature effects included. The fit yields the value of the curvature needed to obtain agreement between the theory and experimental data. We find a value of $+14$ μm for the effective radius [radius $\equiv$(curvature)$^{-1}$] which should be compared with the true radius of 6 μm. In order to explain this difference, one could imagine that the surface of the fiber is

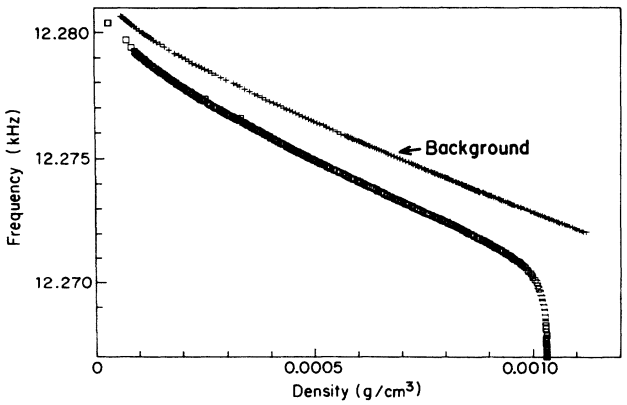

FIG. 3. Resonant frequency of the fiber vs gas density in the cell. The top set of data (crosses) is the hydrodynamic background as described in the text. The lower set of data (squares) is due to hydrodynamic loading and film adsorption combined.

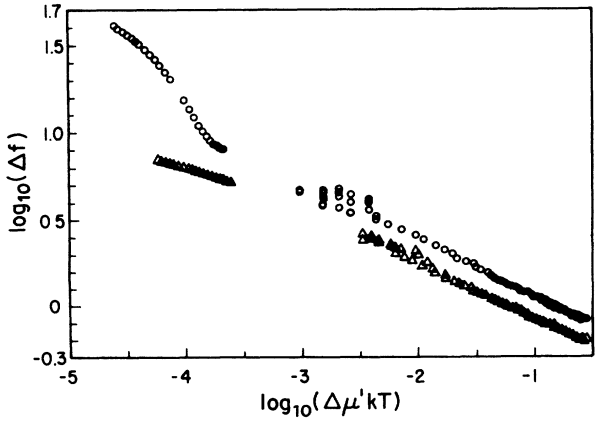

FIG. 4. Frequency shift vs chemical potential difference for the two fibers. Open circles refer to the Fortafil fiber (negative curvature) while the open triangles refer to the P-100 fiber (positive curvature).

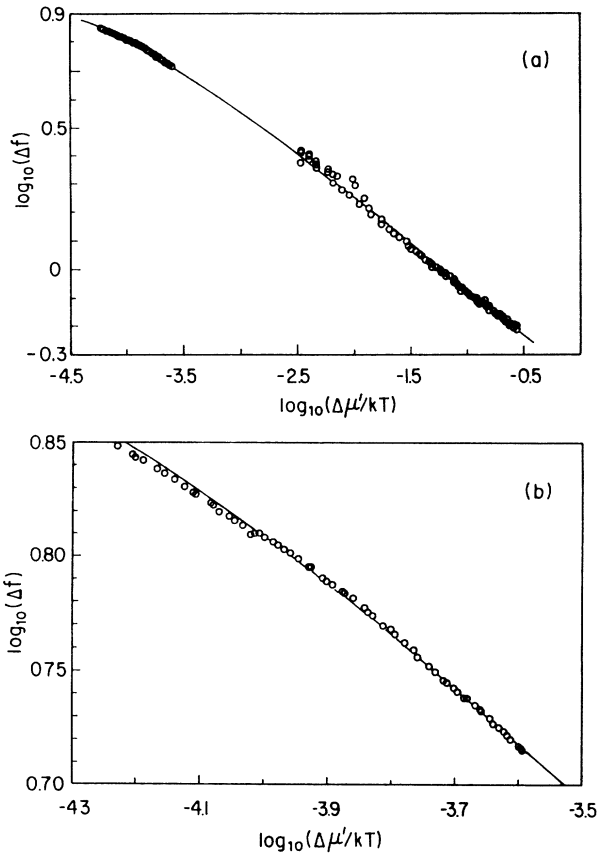

FIG. 5. (a) Frequency shift vs chemical potential difference for the P-100 fiber. Solid line is the fit the DLP theory with an effective curvature. (b) Magnification of the data in the saturated regime.

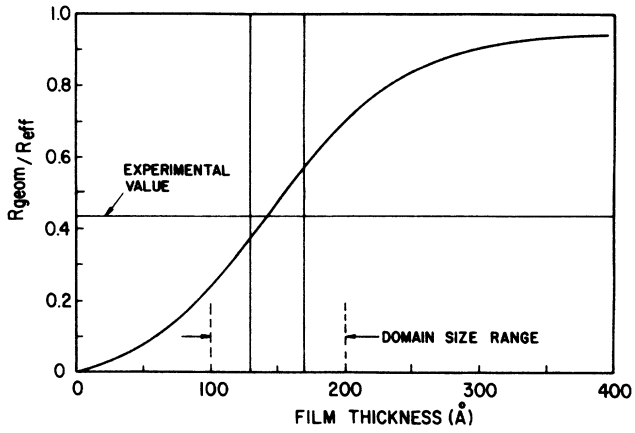

FIG. 6. Qualitative illustration of the dependence of the effective radius of curvature on the film thickness. The two solid vertical lines show the range of film thickness in the saturated regime which determines the effective curvature through our fit to the DLP theory. The fitted value of the curvature is indicated by the horizontal line. The dashed vertical lines show the estimated range of domain sizes on the surface of the fiber.

comprised of flat (faceted) as well as rounded portions. The film thickness on flat areas will be larger and the resulting average thickness will also be larger than what one would expect for a uniformly curved surface having the geometrical radius. There is, however, no reason to expect the functional dependence of d on $\Delta\mu'$ to remain the same as given in Eq. (2), albeit with a different value of radius r.

To see how this might come about, we present the following argument. In the monolayer regime, the effective curvature is zero, since locally the surface always looks flat. At the other extreme, when the film is very thick, we expect that the fine structure of the fiber's surface will not be reflected at the free surface of the film.[18] In this limit, the curvature is determined by the macroscopic radius of the fiber. The exact way in which a crossover between these two limits takes place will be determined by the details of the surface structure. It seems reasonable to expect that this crossover will occur at a film thickness which is of the order of the average domain size of the facets comprising the surface of the fiber. In our case, this is on the order of 100–200 Å. We sketch this qualitative picture in Fig. 6. The data we use in the fit (in Fig. 5) to obtain the curvature cover film thickness between 130 and 170 Å, which, according to this picture, are somewhere in the crossover region. The fitted curvature, having a value of about one-half of the geometrical one is consistent with this fact. The use of a single value of the curvature makes sense only if the curve in Fig. 6 describing the real fiber is not steep in the crossover region.

In Fig. 7, we plot the Fortafil data, along with a fit (dashed line) to Eq. (2) using the minimum (negative) radius of curvature as measured from the electron micrograph of the fiber. Since the concave region of the fiber represents only about 20% of the total surface area, using this radius in Eq. (2) overestimates the enhancement of the film thickness due to curvature. However, it is this

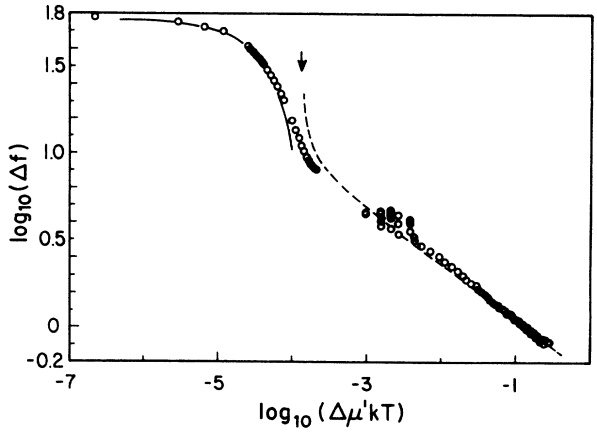

FIG. 7. Frequency shift vs chemical potential difference for the Fortafil fiber. Dashed line is the fit to the DLP theory using the maximum negative curvature measured from the microscope photographs. The solid line shows the calculated frequency shift based on the gradual filling of the concave region of the Fortafil fiber. The arrow indicates the value of the chemical potential difference at which the concave region starts to fill.

minimum radius which determines the value of the chemical potential $\Delta\mu'$ at which the film thickness should diverge. This point is indicated in Fig. 7 by the arrow. The experimental film thickness does not diverge as predicted by the theory. This is understood by realizing that the helium film can fill in the region of negative curvature in such a way as to reduce the curvature. This process is fully reversible.[19] (This is not true for a region of uniform curvature such as the interior of a capillary, where the growth of the film must increase the curvature, and irreversible condensation occurs.[7]) When the liquid level is at a distance h below the fiber, the film will fill in the concave region until the radius of the free surface is just equal to $\sigma v/mgh$. Using this criterion, which we illustrate graphically in Fig. 8, we determine the contribution to the frequency shift due to the mass of the liquid in the filled in region. This is plotted in Fig. 7 (solid line). Once this filling begins, its contribution quickly increases to become the dominant term in the frequency shift. The fit to the data contains no adjustable parameters, nor does it include the effective surface area correction discussed earlier. In particular, the limiting frequency shift observed, just before the fiber is covered with liquid, corresponds to the entire concave area filled with liquid. This represents a film thickness of over 10 000 Å, which is almost two orders of magnitude larger than has been measured elsewhere[10] for helium adsorbed on graphite. Our observation of continuous growth of film spanning from atomic thickness up to 10 000 Å constitutes a conclusive proof of complete wetting of graphite by liquid ^{4}He.

Finally, we would like to address the question of the effective area of the fiber. In order that the fiber have an effective area which is roughly three times the actual geometric one, a considerable portion of the surface must be in the form of holes, cracks, etc. Each hole or crack is a region with a negative radius of curvature. The value of $\Delta\mu'$ at which capillary condensation occurs in a hole of some radius r is determined by $r \leq r_c$, is given by

$$r_c = \frac{\sigma v}{\Delta\mu'} . \tag{8}$$

The range of $\Delta\mu'$ in our experiment corresponds to 20 Å $< r_c < \infty$. This means that at the outset, all the holes with $r < 20$ Å are already filled with liquid. Holes of larger radii must necessarily exist to account for the extra surface area. During the adsorption process, all the holes on the surface with greater values of r_c should fill with liquid. (We emphasize that the filling of holes depends only on $\Delta\mu'$ and not on the ratio of the film thickness to the hole size. This ratio may be very small when a given hole begins to fill. For example, prior to the filling of the concave region of the Fortafil fiber, for which $r_c = 3.5\mu$m, the film thickness is only of the order of 200 Å.)

The net result is that the film growth combines uniform adsorption with the condensation process such as we just described. This issue was raised previously by several authors in a similar context.[3,8] We therefore find it quite amazing that we can represent our data accurately with the DLP theory and an effective surface area. We offer no solution to the puzzle as to why this theory provides an accurate effective representation to the true picture.

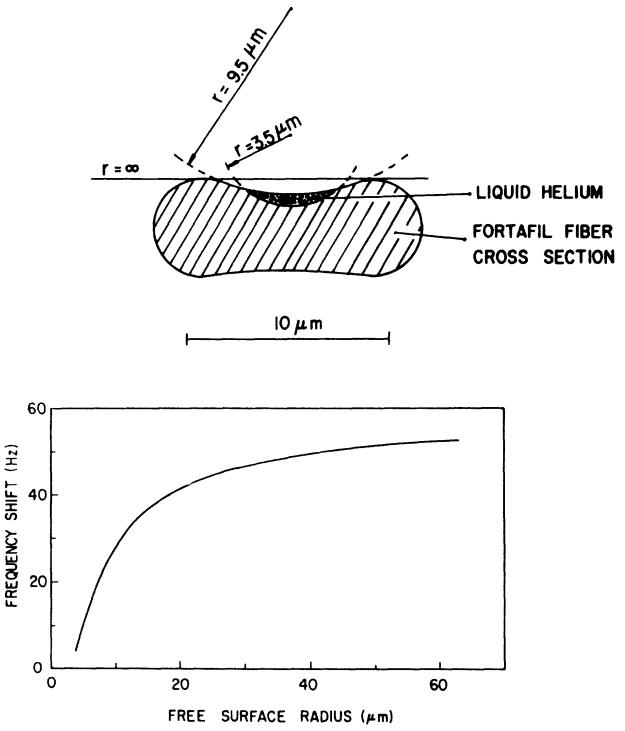

FIG. 8. Top: Cross section of the Fortafil fiber showing the geometrical construction used to calculate the amount of liquid in the concave region for a given critical radius r_c. Bottom: The resulting frequency shift of the fiber against r_c. The result of this calculation is compared with the experimental data in Fig. 7.

CONCLUSIONS

In conclusion, we demonstrated the complete wetting of ^{4}He film on graphite. The role of the curvature of the surface was shown to play an important role on the film growth near saturation conditions. Finally, we addressed the applicability of the DLP theory to the adsorption of the film growth on realistic surfaces.

ACKNOWLEDGMENTS

We would like to thank Steve Lipson for his interest and comments on the manuscript, Mordecai Ayalon for his technical assistance, Steve Gregory for helpful discussions and providing us with the fibers, and David Andelman for his insights and discussion. This work was supported in part by the U.S.–Israel Binational Science Foundation and the Israel Academy of Basic Science. One of us (L.W.) received support from The Lady Davis Foundation.

[1]P. G. de Gennes, Rev. Mod. Phys. **57**, 227 (1985).
[2]R. Pandit, M. Schick, and M. Wortis, Phys. Rev. B **26**, 5112 (1982).
[3]D. F. Brewer, in *The Physics of Liquid and Solid Helium*, edited by K. Benneman and J. Ketterson (Wiley, New York, 1978), Part II, p. 573.
[4]C. Ebner, W. F. Saam, and A. K. Sen, Phys. Rev. B **32**, 1558 (1985).
[5]I. E. Dzyaloshinskii, E. M. Lifshitz, and L. P. Pitaevskii, Adv. Phys. **10**, 165 (1961).
[6]E. S. Sabisky and C. H. Anderson, Phys. Rev. A **7**, 790 (1973).
[7]D. D. Awschalom, J. Warnock, and M. W. Shafer, Phys. Rev. Lett. **57**, 1607 (1986).
[8]M. Bienfait, J. G. Dash, and J. Stoltenberg, Phys. Rev. B **21**, 2765 (1980).
[9]C. E. Bartosch and S. Gregory, Phys. Rev. Lett. **54**, 2513 (1985).
[10]G. Zimmerli and M. H. W. Chan, Phys. Rev. B **38**, 8760 (1988).
[11]L. Bruschi, G. Torzo, and M. H. W. Chan, Europhys. Lett. **6**, 541 (1988).
[12]J. Frenkel, *Kinetic Theory of Liquids* (Oxford, New York, 1949); G. D. Halsey, Jr., J. Chem. Phys. **16**, 931 (1948); T. L. Hill, *ibid.* **17**, 590 (1949).
[13]P-100 fibers are manufactured by Union Carbide.
[14]Fortafil fibers are manufactured by Great Lakes Carbon Inc.
[15]E. Cheng and Milton W. Cole, Phys. Rev. B **38**, 987 (1988).
[16]G. G. Stokes, *Mathematical and Physical Papers* (Cambridge University Press, London, 1922), Vol. 3, p. 38.
[17]Strictly speaking, there is also a correction which must be applied to take into account that the viscosity is temperature dependent, and thus changes during this process. Since the temperature is a weak function of ρ_v, this correction turns out to be rather small, and we have chosen to neglect it in our analysis.
[18]D. Andelman, J. F. Joanny, and M. O. Robbins, Europhys. Lett. **7**, 731 (1988).
[19]S. J. Gregg and K. S. W. Sing, *Adsorption, Surface Area and Porosity* (Academic, London, 1982), p. 129.

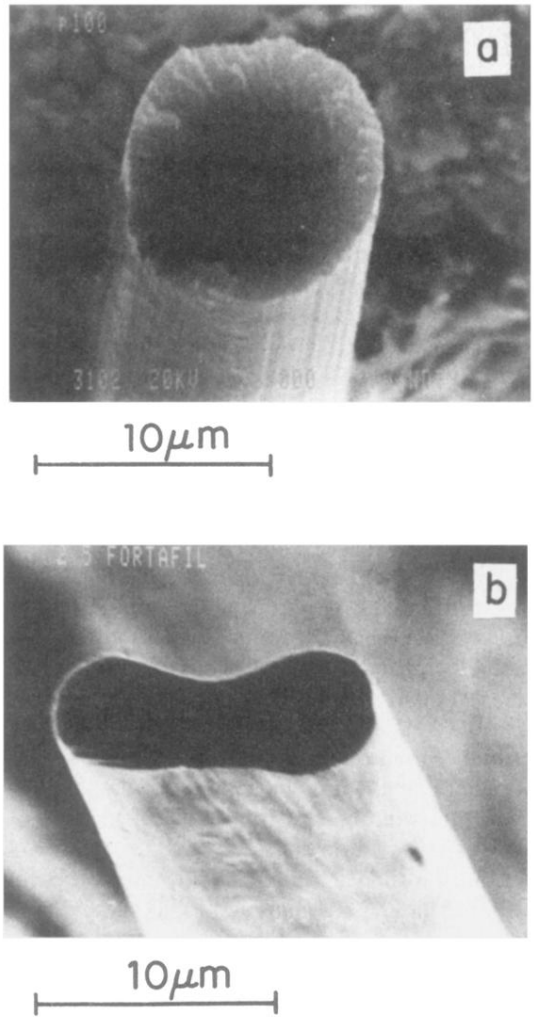

FIG. 1. Scanning electron microscope cross-sectional photographs of the two fibers used in the experiment. (a) P-100 fiber. (b) Fortafil fiber.